

# Quasielastic Light Scattering and Viscoelasticity of Polystyrene in Diethyl Phthalate

C. H. Wang\* and X. Q. Zhang

Department of Chemistry, University of Nebraska, Lincoln, Nebraska 68588-0304

Received August 24, 1992; Revised Manuscript Received November 2, 1992

**ABSTRACT:** A comprehensive quasielastic light scattering study of polystyrene (PS) in diethyl phthalate has been carried out. The homodyne intensity-intensity correlation function of the scattered light is measured as a function of polymer concentration and molecular weight. In the semidilute and concentrated concentration regimes, the time correlation function deviates from a single-exponential shape. The deviation is interpreted as arising from two types of modes, one associated with cooperative diffusion and the other with the viscoelasticity of the polymer solution. The experimental results are interpreted in terms of a recently developed hydrodynamic theory without assuming the transient gel model of de Gennes and Brochard. The concentration dependence of the osmotic modulus is obtained from the static light scattering experiment. Using both theory and experiment, we have obtained the osmotic modulus, the cooperative diffusion coefficient, the longitudinal modulus, and the friction coefficient as a function of polymer concentration. This work furnishes an alternative point of view for the interpretation of the dynamic light scattering data of the polymer solution in the semidilute and concentrated regimes.

## I. Introduction

Mechanical relaxation and dynamic light scattering are techniques that are intimately related. Efforts have been made to correlate structural and dynamic data of a polymer liquid obtained by dynamic light scattering with that by the mechanical relaxation spectrum. Making the correlation not only helps in understanding the light scattering spectrum but also facilitates the unification of the information obtained separately by the two techniques; in addition, it allows the use of one technique to study the polymer liquid when the other becomes restricted or fails. In recent years some progress has been made in this direction. In the bulk polymer melt, the density-density time correlation function is shown to be equivalent to the relaxational bulk longitudinal creep compliance.<sup>1</sup> A recent paper also deals with the depolarized scattering spectrum with reorientational dynamics and shear modulus.<sup>2</sup> Some attempts have recently been made to correlate the quasielastic light scattering (QELS) spectrum with the mechanical relaxation spectrum of the polymer solution.<sup>3,4</sup>

Dynamic light scattering from a dilute polymer solution of a monodisperse molecular weight polymer is characterized by an essentially single-exponential decaying autocorrelation function if the amplitude of the scattering vector  $q$  is sufficiently small such that  $qR_g < 1$ , where  $R_g$  is the mean radius of gyration of the macromolecules in solution. The exponential decay is due to translational diffusion of polymer in the solvent.<sup>5</sup> Increasing the polymer concentration beyond the overlap concentration, defined by  $C^* = M/[(4/3)\pi R_g^3]N_A$ , results in major deviations from the single-exponential decay in the autocorrelation function of the scattered light.<sup>6-16</sup> Here  $N_A$  is the Avogadro constant and  $M$  is the molecular weight. The overlap concentration  $C^*$  separates the dilute regime from the semidilute regime. Above  $C^*$ , neighboring chains begin to overlap, and the hydrodynamic interaction is screened. The deviation from the single-exponential decay is prominent in semidilute solutions with marginal or  $\theta$ -solvents. In the semidilute solution, the QELS spectrum is interpreted as due to scattering from more than one relaxation mode. One of the modes is attributed to the mutual diffusion  $D_m(c)$ , which depends on the polymer concentration and is related to the hydrodynamic corre-

lation length  $\zeta_H$  by

$$D_m(c) = \frac{k_B T}{6\pi\eta_s \zeta_H} \quad (1)$$

where  $k_B$  is the Boltzmann constant,  $T$  is the temperature, and  $\eta_s$  is the viscosity of the solvent. The existence of the other modes has been the subject of much discussion.<sup>6,15-21</sup> We have recently carried out a theoretical analysis using generalized hydrodynamics, with the object of clarifying the nature of the dynamic light scattering spectrum of a binary solution at various concentrations. We have shown that the other modes are due to the effect of viscoelasticity; the transient gel model<sup>17</sup> of de Gennes is a special case of the generalized hydrodynamics calculation.

In this paper, we report experimental results of a comprehensive dynamic light scattering study of a polymer solution consisting of polystyrene (PS) in diethyl phthalate (DEP) as a function of polymer concentration at several molecular weights of PS. We show how the experimental results can be interpreted in terms of the recently developed theory.<sup>3,4</sup> The interpretation is to be contrasted with that previously advanced by Brochard.<sup>22</sup> No assumption of entangled chains or a transient gel model is needed in our interpretation of the QELS spectrum of the semidilute or concentration solution. The difference in the interpretation between the present approach and those previously offered is described in more detail in a review article by one of the authors.<sup>23</sup>

The outline of this paper is as follows. In section II, we review the theoretical background needed in the interpretation of the experimental results. The experimental detail is described in section III. A discussion of the experimental results is given in section IV, which is followed by a summary and conclusion in section V.

## II. Theoretical Background

Using generalized hydrodynamics, it is shown in refs 3 and 4 that the concentration and density fluctuations in a binary solution are, in general, mixed. If the stress tensor of the polymer solution is assumed to be the sum of the partial stress tensor from the polymer component and that from the low molecular weight solvent, then we obtain a

coupled equation for the concentration and density fluctuations as<sup>3</sup>

$$\frac{\partial^2}{\partial t^2}(\delta\rho_2) = \frac{1}{\rho_0} \int_0^t dt' M(t-t') \frac{\partial}{\partial t'} (\nabla^2 \delta\rho) - \frac{\eta_1}{\rho_0} \frac{\partial}{\partial t} (\nabla^2 \delta\rho) + \rho_2 \nabla^2 \mu_2 - \rho_2 \nabla \cdot \mathbf{F}_2 \quad (2)$$

where  $M(t)$  is the longitudinal modulus of the solution equal to  $\{K(t) + (4/3)G(t)\}$  and  $\eta_1$  is the longitudinal viscosity of the solvent equal to  $[\kappa_1 + (4/3)\eta_1]$ .  $\delta\rho_2$  is the fluctuation in the polymer concentration (in g/cm<sup>3</sup>),  $\delta\rho$  is the fluctuation in the polymer density (in g/cm<sup>3</sup>), and  $\rho_0$  is the equilibrium solution density.  $\mu_2$  is the chemical potential (the Gibbs free energy per unit mass) of the polymer component in solution.  $\mathbf{F}_2$  is the average frictional force per unit mass exerted on the polymer by the solvent molecules.

The equations for the frictional force  $\mathbf{F}_2$  and for the chemical potential  $\mu_2$  are given by<sup>3</sup>

$$\nabla \cdot (\rho_2 \mathbf{F}_2) = \xi \frac{\partial}{\partial t} (\delta\rho_2) \quad (3)$$

and

$$\rho_2 \nabla^2 \mu_2 = \phi_2 v_T^2 \nabla^2 \rho + \left[ \phi_1 \left( \frac{\partial \Pi}{\partial \rho_2} \right)_{P,T} - v_T^2 \phi_2 \left( \frac{\partial \rho}{\partial \rho_2} \right)_{P,T} \right] \nabla^2 (\delta\rho_2) \quad (4)$$

where  $\xi = (\rho_0/M_1 M_2) \xi_{12}$ .  $\xi_{12}$  is the friction coefficient and is given in terms of the intermolecular potential;  $\Pi$  is the osmotic pressure, and  $\phi_1$  and  $\phi_2$  are the volume fractions of the solvent and polymer, respectively.

Equation 2 and the auxiliary equations (3) and (4) form a set of equations needed for the calculation of the dynamic light scattering spectrum of a binary polymer solution at all concentrations.

We can separate the isothermal part of the density fluctuation in eqs 2 and 4 into two parts:

$$\delta\rho = \left( \frac{\partial \rho}{\partial \rho_2} \right)_{P,T} \delta\rho_2 + \left( \frac{\partial \rho}{\partial p} \right)_{\rho_2,T} \delta p \quad (5)$$

where the coefficient of the second term is related to the isothermal sound velocity. When dealing with the quasielastic light scattering spectrum, the pressure fluctuation term and the inertia term (the term on the left-hand side of eq 2) can be neglected. These terms do not contribute to the QELS spectrum, as they are the high-frequency terms. After neglecting these terms, one can obtain from eqs 2–4 using standard techniques an expression for the spectral power density of the scattered light associated with concentration fluctuations as

$$I(q, \omega) = \langle |\delta\rho_2(q)|^2 \rangle S(q, \omega) \quad (6)$$

where  $q$  is the amplitude of the scattering vector given by  $q = 4\pi n \sin(\theta/2)/\lambda$ ;  $\theta$  is the scattering angle,  $n$  is the refractive index of the solution, and  $\lambda$  is the wavelength of the incident light in vacuum.  $S(q, \omega)$  is the dynamic structure factor which determines the spectrum of the scattered light and is given by

$$S(q, \omega) = \text{Re} \left[ \frac{\hat{m}(\omega) + \xi}{\Delta(\omega)} \right] \quad (7)$$

where

$$\Delta(\omega) = i\omega \hat{m}(\omega) + \phi_1 q^2 \left( \frac{\partial \Pi}{\partial \rho_2} \right)_{P,T} + i\omega \xi \quad (8)$$

Here, the quantity  $\hat{m}(\omega)$  is given by

$$\hat{m}(\omega) = \frac{q^2}{\rho_0} \left( \frac{\partial \rho}{\partial \rho_2} \right)_{T,P} \int_0^\infty dt e^{-i\omega t} M(t) \quad (9)$$

We note in eq 9 that the longitudinal modulus  $M(t)$  entering into the concentration fluctuation equation is modified by the factor  $(\partial \rho / \partial \rho_2)_{T,P}$ . It is easy to show that this factor is equal to  $(V_1 - V_2)/V_1$ , where  $V_1$  and  $V_2$  are the partial specific volumes of the solvent and solute, respectively. Since  $\hat{m}(\omega)$  must be positive but  $(\partial \rho / \partial \rho_2)_{T,P}$  may be either positive or negative, depending on whether adding polymer is to increase or decrease the solution density, we introduce a coupling parameter  $\beta$ , equal to the absolute value of  $(\rho_2^0 / \rho_0) (\partial \rho / \partial \rho_2)_{T,P}$  to determine the effectiveness in the coupling of the concentration fluctuation to the viscoelasticity of the polymer solution. A strong coupling between concentration and density, hence viscoelasticity, is expected if there is a large difference in the partial specific volumes of the polymer and solvent components in the solution. On the other hand, in the case that  $V_1 \simeq V_2$ , one expects a negligible coupling between the concentration fluctuation and the viscoelasticity of the binary polymer solution. Thus, owing to the coupling parameter  $\beta$ , the concentration fluctuation in the polymer solution does not see the full impact of the longitudinal stress  $M(t)$ , rather only  $\beta M(t)$ .

The dispersion relationship of the concentration fluctuation dynamics is determined by the function  $\Delta(\omega)$ , which, according to eq 8, is determined by the osmotic modulus  $M_\Pi$ , given by  $\phi_1 \rho_2^0 (\partial \Pi / \partial \rho_2)_{T,P}$ , the friction coefficient  $\xi$ , and the frequency dependence of the dynamic longitudinal modulus of the polymer solution, given by

$$M^*(\omega) = i\omega \int_0^\infty dt e^{-i\omega t} M(t) = M'(\omega) + iM''(\omega) \quad (10)$$

where  $M'(\omega)$  and  $M''(\omega)$  are the real and imaginary parts of the longitudinal modulus, respectively.

Equation 7 is an important result. It describes the effect of the viscoelasticity of the polymer solution on the QELS spectrum owing to the concentration fluctuation. Clearly, according to eqs 7 and 8, in addition to the osmotic pressure fluctuation, the viscoelastic response, as described by  $M(t)$ , also plays a role in affecting the QELS spectrum. Nevertheless, in contrast to the bulk polymer case,<sup>1</sup> it should be emphasized that the concentration fluctuation spectrum in a binary solution does not see the full stress modulus  $M(t)$ , but only  $\beta M(t)$ . Only for the polymer solution with a nonvanishing  $\beta$  parameter can the viscoelastic relaxation behavior affect the QELS spectrum.

Since the longitudinal stress modulus has a wide distribution of relaxation times, we expect an extensive mixing between the viscoelastic relaxation process and the osmotic pressure fluctuation in the 10<sup>-1</sup>–10<sup>6</sup>-Hz frequency range for binary solutions with a large  $\beta$ . In such systems, we anticipate observing a rather complex QELS spectrum in the polymer solution.

The stress relaxation modulus can, in general, be written as

$$M(t) = \sum_i M_i e^{-t/\tau_i} \quad (11)$$

Thus, the dynamic modulus becomes

$$M^*(\omega) = \sum_i \left( M_i - M_i \frac{1}{1 + i\omega\tau_i} \right) \quad (12)$$

where  $M_i$  is the amplitude of the relaxation mode of the longitudinal modulus with the relaxation time  $\tau_i$ .

One notes from eq 12 that for the rapidly relaxing system in which  $\omega\tau_i \ll 1$  applies to all relaxation modes, the dynamic longitudinal modulus is small. For such systems, the viscoelastic effect is small and the QELS spectrum is determined mainly by the osmotic pressure fluctuation. More interesting is the case where  $\omega\tau_i \geq 1$ , the case relevant to polymer solutions in the semidilute and concentrated regimes. For systems satisfying this condition, the viscoelastic response of the polymer solution is expected to be present in the QELS spectrum.

Using a perturbation technique, it has been shown that for the systems in which  $\omega\tau_i \geq 1$ , the normalized autocorrelation function of concentration fluctuations  $g(q,t)$  is given by<sup>4</sup>

$$g(q,t) = \frac{\langle \delta\rho_2(q,t)\delta\rho_2^*(q) \rangle}{\langle |\delta\rho_2(q)|^2 \rangle} = Ae^{-D_c q^2 t} + \sum_i B_i e^{-t/\tau_i} \quad (13)$$

where  $g(q,t)$  is related to the dynamic structural factor  $S(q,\omega)$  by a Fourier transformation;  $D_c$  is the cooperative diffusion coefficient given by<sup>27</sup>

$$D_c = [\phi_1(\partial\Pi/\partial\rho_2)_{P,T} + \beta M_0/\rho_2^0]/\xi \quad (14)$$

Equation 13 shows that the time correlation function is bifurcated into two groups: one consists of a single-exponential decay with the decay rate given by  $D_c q^2$ , and the other consists of a group of viscoelastic relaxation modes associated with relaxation time constants  $\tau_i$ , which are the longitudinal stress relaxation times. Note that the time constant of the single-exponential decay term depends on  $q^2$  and the relaxation times of the viscoelastic modes are independent of  $q$ . The amplitude factors  $A$  and  $B_i$  are, in general,  $q$  dependent; however, in the large wave vector region such that  $D_c q^2 \gg \tau_i^{-1}$ , the amplitude factors  $A$  and  $B_i$  are given by<sup>24</sup>

$$A = 1 - \beta M_0/(\beta M_0 + M_\Pi) \quad (15a)$$

and

$$B_i = \beta M_i/(\beta M_0 + M_\Pi) \quad (15b)$$

where  $M_\Pi = \phi_1 \rho_2^0 (\partial\Pi/\partial\rho_2)_{P,T}$  is the osmotic modulus and  $M_0 = \sum_i M_i$  is the amplitude of the total longitudinal stress modulus.

The theory summarized by eqs 13–15 will form the basis with which we shall use to interpret and discuss the present experimental results.

### III. Experimental Section

The polystyrene (PS) samples used in this study were purchased from Toya Soda and have polydispersity indexes  $\bar{M}_w/\bar{M}_n$  ranging from 1.01 to 1.03. These PS samples are nearly monodisperse. Polymer solutions were prepared by dissolving PS in diethyl phthalate (DEP) solvent (Pfaltz and Bauer, Inc.). Dust in solutions with less than 1 wt % PS was removed by filtering the solution through 0.2- $\mu$ m Millipore filters into the light scattering cell. Solutions with higher concentration are difficult to filter, and dust in these solutions was removed by centrifugation for more than 8 h at 9000g.

Static light scattering (SLC) measurements were performed by using an apparatus consisting of a Brookhaven 200 SM goniometer and a Spectra-Physics 125 He-Ne laser with a power of 40 mW at the wavelength of 632.8 nm.

The refractive index increment  $dn/dc$  of PS in DEP is 0.094 at the wavelength of 632.8 nm (Brandrup, J.; Immergut, E. M. *Polymer Handbook*; Interscience: New York, 1966) at 20 °C. We assume that this value does not change with concentration. The coupling parameter  $\beta$  is determined from the density measurement. The densities of the polymer solutions were determined by using volumetric flasks and a weight balance. Pyrex Class A

5- and 10-mL volumetric flasks fit with Pyrex stoppers were used. The precision of the balance is  $\pm 0.0001$  g.

The radius of gyration  $R_g$  and the second virial coefficient  $A_2$  were determined from a Zimm plot according to the conventional method. The radius of gyration data were used to calculate the overlap concentration  $C^*$ .

Dynamic light scattering (DLS) measurements were carried out using an apparatus consisting of a Brookhaven 200 SM goniometer and a Brookhaven BI-2030 digital correlator. The light source is an argon ion laser operating at 488.0 nm with 150-mW power. The DLS correlation functions obtained at the scattering angle  $\theta = 90^\circ$  from the Brookhaven BI-2030 correlator equipped with a multiple sample times option were compared with those obtained by an ALV-5000 logarithmically spaced correlator covering  $10^{-6}$  to  $3 \times 10^2$  s. Samples were measured at various scattering angles ranging from 30 to  $150^\circ$ . All measurements were made at 23 °C.

The normalized correlation function  $g(q,t)$  is obtained from the intensity–intensity autocorrelation function,  $G(q,t)$ , via the Sigert relation:

$$g(q,t) = [G(q,t)/A - 1]^{1/2} \quad (16)$$

where  $A$  is the experimentally determined baseline. For all DLS experiments the measured baseline  $A$  is in agreement with the theoretically calculated baseline to within 5%.

Two procedures are used to analyze the  $g(q,t)$  versus  $t$  data. One involves using the CONTIN program in which  $g(q,t)$  is decomposed into a distribution of relaxation modes given by<sup>28</sup>

$$g(q,t) = \sum_i A_i e^{-t/\tau_i} \rightarrow \int_0^\infty \rho(\tau) e^{-t/\tau} d\tau \quad (17)$$

where  $\rho(\tau)$  measures the distribution on the relaxation time  $\tau$ . The second data analysis method utilizes a double Kohlraush–Williams–Watts (KWW)-stretched exponential function given by

$$g(q,t) = x_1 \exp[-(t/\tau_1)^{\beta_1}] + x_2 \exp[-(t/\tau_2)^{\beta_2}] \quad (18)$$

The mean relaxation times are calculated by using

$$\bar{\tau}_i = \tau_i \frac{\Gamma(1/\beta_i)}{\beta_i}, \quad i = 1 \text{ or } 2 \quad (19)$$

where  $\tau_i$  is the characteristic relaxation time;  $\Gamma(x)$  is a  $\Gamma$  function. The parameter  $x_i$  measures the strength of mode  $i$ ; clearly,  $x_1 + x_2 = 1$ , as  $g(q,t)$  is normalized at  $t = 0$ . The mean relaxation times calculated by the CONTIN method and the double KWW fit agree to within 10%.

### IV. Results and Discussion

Polarized QELS measurements have been made in the homodyne mode to characterize the dynamic behavior of PS solutions in DEP as a function of PS concentration and molecular weight. The homodyne time correlation function  $G(q,t)$  is theoretically related to  $g(q,t)$  according to eq 16; in practice, however, one needs to introduce a contrast factor  $b$  to account for the contrast reduction due to the finite pinhole size used and the limited dynamic range of the digital correlator, which can only effectively probe dynamic events at times longer than  $10^{-6}$  s. For this reason, the measured initial amplitude of  $g(q,t)$  at  $t = 0$  needs to be divided by the contrast factor  $b$  to achieve the normalization. A representative time correlation function of PS solution in DEP with a PS concentration equal to 0.1025 g g<sup>-1</sup> obtained at  $90^\circ$  is shown in Figure 1. The correlation functions obtained in this work were mostly carried out with the BI-2030 correlator, because our BI-2030 correlator is equipped with a goniometer, which makes it convenient to do the angular-dependent measurement. However, as mentioned above, we have compared the correlation functions obtained at  $90^\circ$  with those obtained with an ALV-5000 correlator, which covers over 8 decades in delay time in one run (Figure 1). The ALV-5000

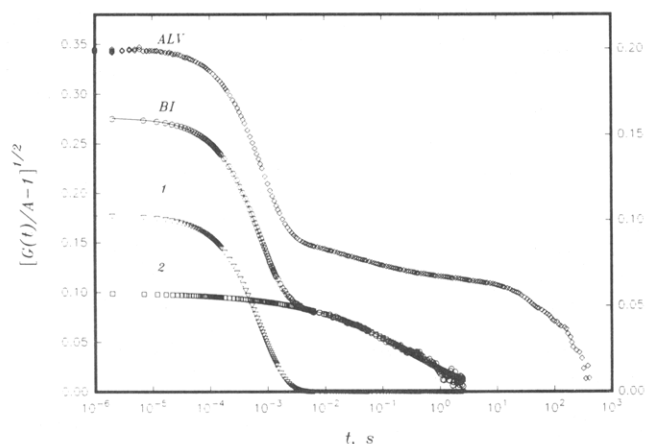


**Figure 1.** Measured time correlation function  $g(q,t)$  of PS in DEP. The molecular weight ( $\bar{M}_w$ ) of PS is  $2.88 \times 10^6$  ( $\bar{M}_w/\bar{M}_n = 1.03$ ) and the concentration is  $0.1025 \text{ g g}^{-1}$ . Curve 1 is the contribution from cooperative diffusion obtained by fitting  $g(q,t)$  to eq 18, and curve 2 is due to the second term.

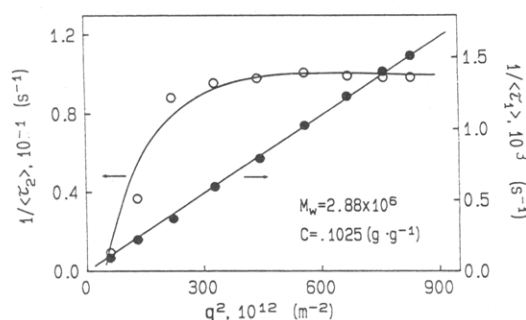


**Figure 2.** Plots of mean relaxation rates  $\langle \tau_1 \rangle^{-1}$  and  $\langle \tau_2 \rangle^{-1}$  for PS solution ( $\bar{M}_w = 2.88 \times 10^6$ ,  $C = 0.1025 \text{ (g g}^{-1}\text{)}$ ) as a function of  $q^2$ . The mean relaxation times  $\langle \tau_i \rangle$  are calculated by using eq 19.

correlator is more convenient than the Brookhaven BI-2030 correlator for the QELS study of the polymer solution in the semidilute and concentrated regimes as the time correlation function  $G(q,t)$  takes more than 4.3 decades in time to decay to the background. The 4.3 decades in delay time is the upper limit of the BI-2030 correlator. However, when three correlation functions separately obtained with the BI-2030 correlator with different sampling times are spliced together, the resultant correlation function  $G(q,t)$  covering 8 decades in delay times becomes practically the same as that obtained with the ALV-5000 correlator in one run. Also shown in Figure 1 is the decomposition of  $G(q,t)$  into two contributions in accordance with the double stretched exponential fit given by eq 18. The fast-decay portion (curve 1) is almost single exponential ( $\beta_1 = 0.99$ ), whereas curve 2 is rather broad ( $\beta = 0.21$ ), covering a dynamic range from  $1 \mu\text{s}$  to over  $100 \text{ s}$ . There is a considerable deviation at long time ( $>100 \text{ s}$ ), due possibly to the artifact of the correlator.

Shown in Figure 2 are the reciprocals of the relaxation times plotted versus  $q$ . The relaxation rate constant of the mode which is single exponential is proportional to  $q^2$ , whereas, except for the values at small  $q$  ( $<17.32 \times 10^{-6} \text{ m}^{-1}$ ), the mean relaxation of the broad nonexponential decay is practically independent of  $q$ . We associate the  $q^2$  dependence mode with cooperative diffusion and the  $q$ -independent modes with the viscoelastic modes. The decrease in the relaxation rate  $1/\langle \tau_2 \rangle$  with  $q$  in the small- $q$  regime is due to the mixing of the cooperative diffusion mode with the viscoelastic modes at small  $q$ , in which the condition  $D_c q^2 \gg \tau_i^{-1}$  ceases to apply.<sup>4</sup>

We have calculated the cooperative diffusion coefficient  $D_c$  by using the formula  $D_c = (q^2 \langle \tau_1 \rangle)^{-1}$ . The cooperative

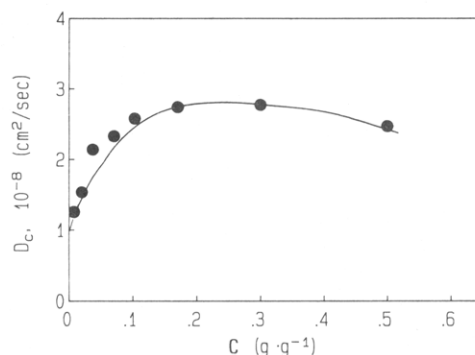


**Figure 3.** Plot of the cooperative diffusion coefficient  $D_c$  as a function of concentration.  $D_c$  is calculated from  $\langle \tau_1 \rangle$  in accordance with the formula  $D_c = [q^2 \langle \tau_1 \rangle]^{-1}$ .

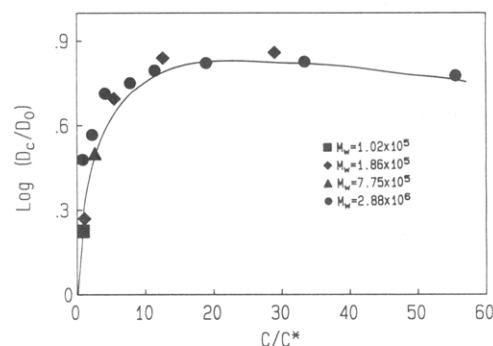


**Figure 4.** Plot of  $\log(D_c/D_0)$  vs  $C/C^*$  for PS in DEP for different PS molecular weights.  $\bar{M}_w$  of samples: (●)  $2.88 \times 10^6$ ; (▲)  $7.75 \times 10^6$ ; (▼)  $1.86 \times 10^6$ ; (■)  $1.02 \times 10^6$ .

diffusion coefficient  $D_c$  is plotted in Figure 3 as a function of concentration for the solutions prepared with  $\bar{M}_w = 2.88 \times 10^6$  ( $\bar{M}_w/\bar{M}_n = 1.03$ ). In the dilute and semidilute concentration regimes,  $D_c$  increases rapidly with increasing polymer concentration. The increase levels off at about 10 times the overlap concentration. It reaches a broad maximum at a concentration about equal to  $0.3 \text{ g g}^{-1}$  ( $\approx 25$  times the overlap concentration) and then it decreases gradually with further increasing concentration. If  $D_c$  is qualitatively identified with the mutual diffusion coefficient, then according to eq 1, the concentration dependence behavior of  $D_c$  indicates that for  $C < 10C^*$ , the hydrodynamic correlation length  $\zeta_m$  decreases rapidly with increasing polymer concentration. The decrease in  $\zeta_m$  with increasing  $C$  has been predicted by scaling theory in good solvent with a power law<sup>18</sup> concentration dependence given by  $\zeta_H \sim C^{-0.75}$ . Our results for  $C < 5C^*$  can be forced to follow a power law, but the exponent is about equal to  $-0.62$ .

PS samples with different molecular weights have also been studied. A more detailed analysis of the molecular weight dependence will be published elsewhere. Here we show the preliminary results. Using the static light scattering technique, we have determined the radius of gyration  $R_g$  for PS in DEP with different PS molecular weights. The overlap concentrations  $C^*$  for different PS molecular weights are then determined. We have normalized  $C$  to  $C^*$  and in Figure 4 have plotted  $\log(D_c/D_0)$  versus  $C/C^*$  for PS with different molecular weights. Here  $D_0$  is  $D_c$  at infinite dilution. When the concentration is normalized to  $C^*$ , the diffusion coefficient ratio  $D_c/D_0$  obtained for PS with different molecular weights falls on a master curve. For  $C/C^* < 10$ ,  $D_c/D_0$  first increases rapidly with increasing concentration, reaches a broad maximum, and then falls off for  $C/C^* > 25$ .

The cooperative diffusion coefficient  $D_c$  is given by eq 14 in terms of osmotic and longitudinal stress moduli. In

the semidilute regime, increasing the polymer concentration also increases the osmotic modulus as well as the longitudinal stress modulus (multiplied by the  $\beta$  parameter); the friction coefficient also increases but to a lesser degree (see later). Thus, in this concentration range, the increase of  $D_c$  with increasing polymer concentration is due to the increase of osmotic and longitudinal moduli. As the osmotic and longitudinal stress moduli reach the plateau values, any further increase in the polymer friction coefficient owing to the increase of polymer concentration leads to a decrease in the cooperative diffusion coefficient.

Brochard<sup>22</sup> has applied scaling theory to discuss the concentration dependence of  $D_c$  in the semidilute regime. In Brochard's theory, entanglements among different polymer chains are assumed to form a transient gel network of lifetime  $\tau_R$ . An additional assumption is that the polymer solution is characterized by only two distinct elastic moduli: the osmotic modulus  $M_\Pi$  and the shear modulus  $G$ . Assuming that the concentration dependences of  $M_\Pi$ ,  $G$ , and the friction coefficient for good solvents are given by  $M_\Pi = K_\Pi C^3$ ,  $G = G_0 C^2$ , and  $\xi = \xi_0 C^2$ , the theory leads to a linear concentration dependence of  $D_c$ :

$$D_c = \frac{4}{3} \frac{G_0}{\xi_0} + \frac{K_\Pi}{\xi_0} C \quad (20)$$

As mentioned above, the prediction of a linear concentration dependence of  $D_c$  is not observed in the present work.

Brochard's theory on  $D_c$  is based upon the assumption of an incompressible fluid. The effect due to the compressional modulus is altogether neglected. It differs considerably from the work reported in refs 2–4, which deals with a compressible fluid, and it includes the mechanical compressional modulus  $K$ . When the compressional modulus is combined with  $G$ , it yields the longitudinal modulus:  $M_0 = K + 4G/3$ . In Brochard's work the coupling parameter  $\beta$  is equal to 1. The role of the solvent is to provide friction to the macromolecule. The contribution of solvent molecules to density and concentration fluctuations is not explicitly considered. As discussed below, the result of  $\beta = 1$  is never realized in polymer solutions because the solvent molecules modify the concentration fluctuation and they need to be taken into account. Using scaling arguments, Brochard gives another prediction:  $M_\Pi/G \gg 1$  for good-solvent solutions and  $M_\Pi/G \approx 1$  for  $\Theta$ -solvent solutions. Although the value of  $K$  is not well known, if one assumes that in the polymer solution  $K$  is of the same order of magnitude as  $G$ , Brochard's prediction is essentially  $M_\Pi/M_0 \gg 1$  for good-solvent solutions and  $M_\Pi/M_0 \approx 1$  for  $\Theta$ -solvent solutions. We now show that this conclusion is incorrect, considering the fact that  $M_\Pi$  is usually several orders of magnitude smaller than the longitudinal stress modulus  $M_0$ . In other words, we expect that  $M_\Pi/M_0$  is always much less than 1 for both types of solutions. In fact, as we shall subsequently show, it is the result of the combination of  $M_0$  with  $\beta$  that renders the viscoelastic contribution to have a comparable value with  $M_\Pi$ . However, despite the fact that one always has  $M_\Pi/M_0 \ll 1$ , we now show that  $M_\Pi/\beta M_0 > 1$  in the semidilute solution; this ratio decreases rapidly with increasing PS concentration, reaching a result of  $M_\Pi/\beta M_0 \approx 1$  at high concentration.

$M_\Pi/M_0$  can be determined by analyzing the shape of the correlation function  $G(q, t)$ . According to eqs 13–15, the amplitude factor associated with the cooperative diffusion term is  $[1 - \beta M_0/(\beta M_0 + M_\Pi)]$ . The double KWW stretched exponential function fit to  $g(q, t)$ , as given by eq 18, allows one to identify the parameter  $x_1$  to be

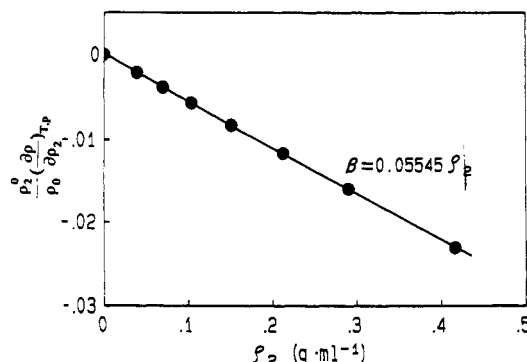


Figure 5. Coupling parameter  $\beta$  plotted versus concentration  $\rho_2$  for the PS sample at 20 °C with  $M_w = 1.86 \times 10^6$ . Over the concentration range from 0 to 0.5 g/mL,  $\beta$  can be represented by  $\beta = -0.055|\rho_2|$ .

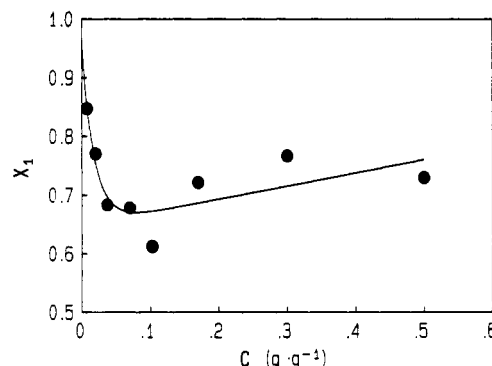


Figure 6. Amplitude factor  $x_1$  of the cooperative diffusion mode plotted as a function of PS concentration.

Table I  
Osmotic Modulus  $M_\Pi$ , Longitudinal Moduli  $M_\Pi$  and  $M_0$ , and  $M_\Pi/M_0$  of PS in DEP

$C$ (g g <sup>-1</sup> )	$M_0/M_\Pi$	$M_\Pi$ (kPa)	$M_\Pi$ (GPa)	$M_0$ (MPa)
0.0076	427.66	0.024	3.64	0.0103
0.020	268.98	0.176	3.67	0.0473
0.037	226.38	0.533	3.73	0.1207
0.07	122.28	2.899	3.85	0.3545
0.103	111.21	7.604	3.99	0.8456
0.17	40.92	14.180	4.39	0.5802
0.30	18.31	(64.327)	5.50	(1.1778)
0.50	13.36	(190.961)	7.09	(2.5512)

equal to

$$x_1 = 1 - \frac{\beta M_0}{\beta M_0 + M_\Pi} = 1 - \frac{\beta}{\beta + (M_\Pi/M_0)} \quad (21)$$

We have determined  $\beta$  by measuring the solution density as a function of polymer concentration. As described in the Experimental Section,  $\beta$  is determined by measuring the overall density of the solution as a function of the polymer concentration. From the slope of the  $\rho$  vs  $\rho_2$  plot, we have obtained  $\beta$  as a function of  $\rho_2$ . The concentration dependence of  $\beta$  is given in Figure 5. The amplitude factor  $x_1$  obtained from the fit of  $g(q, t)$  to eq 18 is shown in Figure 6 as a function of polymer concentration. Having obtained  $x_1$ , we use the measured  $\beta$  value to calculate  $M_0/M_\Pi$  as a function of concentration by employing eq 21. The results for  $M_\Pi/M_0$  calculated as a function of polymer concentration are given in Table I. One notes that at low concentration,  $M_0$  is more than 2 orders of magnitude larger than  $M_\Pi$ .  $M_0/M_\Pi$  decreases with increasing polymer concentration. At  $C = 0.5$  g g<sup>-1</sup>,  $M_0$  is still more than 13 times the value of  $M_\Pi$ . The increase in  $M_\Pi/M_0$  (or decrease in  $M_0/M_\Pi$ ) is due to a more rapid increase in the osmotic modulus as the polymer concentration increases. In the semidilute concentration  $M_0$  is several hundred times

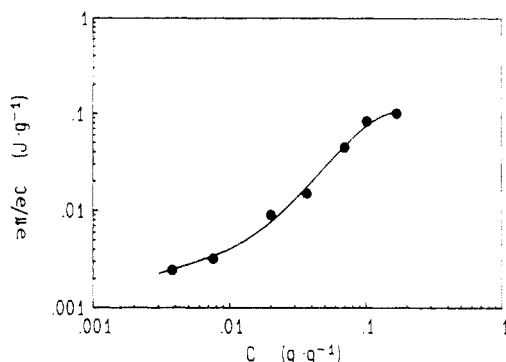


Figure 7. Inverse osmotic compressibility  $(\partial\Pi/\partial c)_{T,P}$  plotted versus  $c$  for PS in DEP.

larger than  $M_{\Pi}$ ; thus we have  $M_{\Pi}/M_0 \ll 1$ , in contrast to the result of  $M_{\Pi}/M_0 \gg 1$  for good-solvent solution predicted by Brochard.

The osmotic modulus  $M_{\Pi}$  can be obtained by using the static light scattering (SLS) technique. The inverse osmotic compressibility,  $(\partial\Pi/\partial c)_{P,T}$ , is equal to the reduced scattering intensity at zero angle  $Kc/R(0)$ , multiplied by  $RT$ . Here  $K$  is an optical constant equal to  $4\pi n_0^2(dn/dc)^2/N_A\lambda^4$ , where  $n_0$  is the solvent refractive index and  $dn/dc$  is the refractive index increment. We have measured the reduced scattering intensity  $Kc/R_{\theta}$  as a function of scattering angle on the same samples as used for the dynamic light scattering measurements. The Rayleigh ratio  $R_{\theta}$  was obtained and calibrated with benzene:  $R_{90} = 8.8 \times 10^{-6}$  at 25 °C.<sup>26</sup> The  $Kc/R_{\theta}$  values at different scattering angles were plotted as a function of  $q$  and then extrapolated to  $q = 0$  to obtain  $Kc/R(0)$ . The inverse osmotic compressibility obtained is shown in Figure 7 as a function of concentration. At low concentration,  $\partial\Pi/\partial c$  can be described by a second virial coefficient ( $A_2$ ), which is equal to  $2.34 \times 10^{-4}$  mol·mL/g<sup>2</sup> for PS in DEP at 23 °C, in comparison with  $A_2 = 2.24 \times 10^{-4}$  mol·mL/g<sup>2</sup> for PS in toluene at 20 °C. Thus, at 23 °C DEP is a good solvent for PS. The rapid increase of  $\partial\Pi/\partial c$  with increasing polymer concentration is due to the large contribution of PS chain repulsions. The transition from dilute to semidilute and then to concentrated solution is gradual without a sharp and identifiable slope change, suggesting that a scaling law is not applicable to  $\partial\Pi/\partial c$  in these concentration regimes. Having obtained the inverse osmotic compressibility, we calculated the osmotic modulus using the expression  $M_{\Pi} = \phi_1(\partial\Pi/\partial\rho_2)\rho_2 = \phi_1(\partial\Pi/\partial c)c$ . The results for  $M_{\Pi}$  at various concentrations are listed in Table I. The osmotic modulus  $M_{\Pi}$  increases rapidly with increasing concentration.<sup>28</sup> With the availability of the  $M_{\Pi}$  data, the value of the longitudinal stress modulus  $M_0$  can now be determined. The  $M_0$  values at various PS concentrations are listed in Table I. The concentration dependences of both  $M_0$  and  $M_{\Pi}$  are also plotted in Figure 8. The concentration dependences of  $M_{\Pi}$  and  $M_0$  can be described by a power law:  $M_{\Pi} \sim C^{\zeta_{\Pi}}$  and  $M_0 \sim C^{\zeta_0}$ , with  $\zeta_{\Pi} = 2.13$  and  $\zeta_0 = 1.67$ .

With the availability of  $M_{\Pi}$ ,  $M_0$ , and  $\beta$ , we can readily calculate  $M_{\Pi}/\beta M_0$ .  $M_{\Pi}/\beta M_0$  plotted as a function of polymer concentration is shown in Figure 9. As mentioned above, although we have  $M_{\Pi}/M_0 \ll 1$  at all polymer concentrations,  $M_{\Pi}/\beta M_0 \gg 1$  at low polymer concentrations; this ratio decreases from 5.0 at  $c = 0.0076$  g g<sup>-1</sup> to about 1.4 at 0.103 g g<sup>-1</sup> and appears to decrease further at higher concentration.  $M_{\Pi}/\beta M_0$  measures the relative strength of the osmotic modulus with respect to the effect of viscoelasticity on the concentration fluctuation. The decrease in  $M_{\Pi}/\beta M_0$  is due mainly to the increase in  $\beta$  as

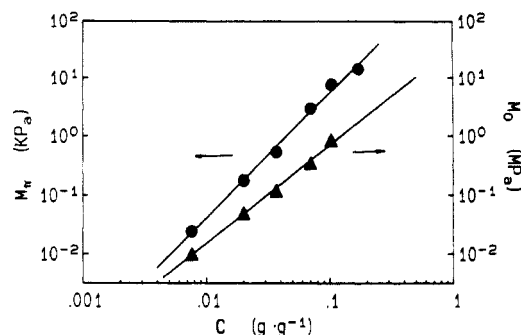


Figure 8. Osmotic modulus  $M_{\Pi}$  and longitudinal stress modulus  $M_0$  plotted versus concentration for PS in DEP.

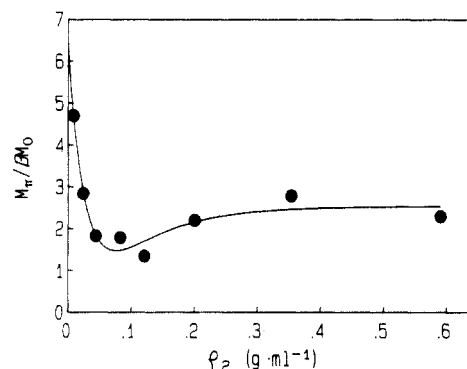


Figure 9.  $M_{\Pi}/\beta M_0$  plotted as a function of concentration.

the polymer concentration increases. Clearly, the coupling parameter plays a crucial role in bringing the full longitudinal stress modulus to a magnitude that is actually involved in the concentration fluctuation. Thus, the effect of the coupling parameter  $\beta$  cannot be neglected.

The longitudinal stress modulus  $M_0$  as determined in the present work from the combined use of the QELS and SLS techniques corresponds to the value at the frequency about equal to  $10^6$  Hz, due to the limitation of the dynamic range of the digital correlator (the shortest reliable delay time of state-of-the-art digital correlators is about 1  $\mu$ s). It is of interest to compare the presently determined  $M_0$  values by QELS with the high-frequency longitudinal modulus  $M_{\infty}$  that can be determined by using the Brillouin scattering technique.

The shift ( $\Delta\nu_B$ ) of the Brillouin doublet due to the scattering of the longitudinal hypersonic wave in the PS solution is related to the high-frequency longitudinal modulus  $M_{\infty}$  by  $\Delta\nu_B = q(M_{\infty}/\rho_0)^{1/2}/2\pi$ .<sup>29</sup> We have measured  $\Delta\nu_B$  as a function of polymer concentration for the PS/DEP solution using a five-pairs Fabry-Perot interferometer. With the help of the solution density data, we have calculated  $M_{\infty}$  as a function of polymer concentration. The  $M_{\infty}$  values are listed in Table I; they are of the same order of magnitude as those obtained for other polymer systems.<sup>29</sup>  $M_{\infty}$  is nearly 5 orders of magnitude higher than  $M_0$  at low polymer concentration and is a factor of  $1.36 \times 10^3$  larger than  $M_0$  at high concentration ( $c = 0.33$  g g<sup>-1</sup>). The large difference between  $M_{\infty}$  and  $M_0$  arises from the relaxation effect. In Brillouin scattering, one measures the response at GHz ( $10^9$  Hz). At this frequency, the system albeit a polymer solution, is glassy, and, hence, it has a high modulus  $M_{\infty}$ . On the other hand, as mentioned above, in QELS the response is at 1 MHz ( $10^6$  Hz) or less; at this frequency, the system is in the liquid or rubbery state, and the dynamics of chain motion as well as the effect of the solvent molecule play an important role in relaxing the longitudinal modulus. The values of  $M_{\infty}$  and



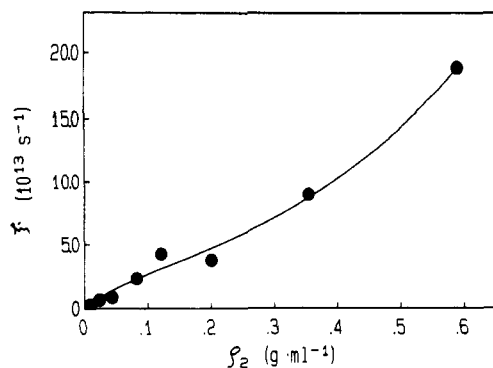


Figure 10. Friction coefficient  $\xi$  of PS in DEP plotted as a function of PS concentration.  $\xi$  is calculated from eq 14.

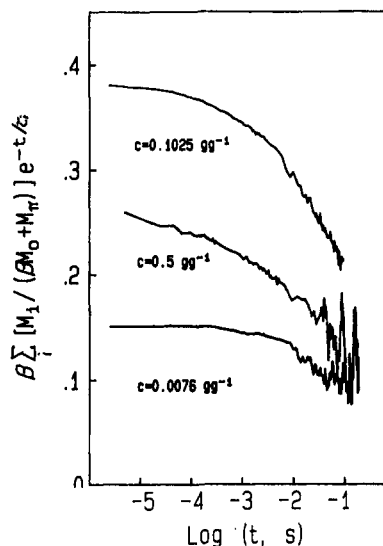


Figure 11. Relaxation of viscoelastic modes as determined by QELS for three PS/DEP samples with different concentrations.

$M_0$  determined in the present work are in qualitative agreement (by having the same order of magnitude) with those determined by the mechanical technique for polymer solution.<sup>30</sup>

Having obtained  $M_\Pi$  and  $M_0$ , we can use them to determine the friction coefficient  $\xi$  from the cooperative diffusion coefficient  $D_c$  data. Using eq 14, we have calculated the friction coefficient  $\xi$ , and the results are plotted in Figure 10 as a function of polymer concentration. The friction coefficient is larger than  $10^{13} \text{ s}^{-1}$ , indicating the rapid interaction of small solvent molecules and the polymer segments on the diffusing polymer chain. As expected, the friction coefficient increases smoothly with increasing concentration.

Finally, we show the viscoelastic contribution to the correlation function  $g(q, t)$ . This is obtained by subtracting from  $g(q, t)$  the contribution due to the cooperative diffusion (cf. eq 13). The correlation functions due to the viscoelastic contribution are shown in Figure 11 for three polymer concentrations. At low concentrations ( $c = 0.0076 \text{ g g}^{-1}$ ), the viscoelastic contribution accounts for about 15% of the short time ( $\approx 10^{-6} \text{ s}$ ) value, but the contribution steadily increases with increasing concentration, reaching about 38% at  $c = 0.1025 \text{ g g}^{-1}$ . One notes that the correlation function associated with the viscoelastic effect has a wide distribution of relaxation times, ranging from  $1 \mu\text{s}$  to greater than  $10^6 \mu\text{s}$ . At short times, it overlaps with the cooperative diffusion mode; thus, referencing the viscoelastic component to a slow mode<sup>13</sup> is misleading.

The viscoelastic modes are always present in the QELS spectrum. The manifestation of the viscoelastic model depends on the amplitude factor  $\beta M_i / (\beta M_0 + M_\Pi)$  as

indicated in eq 15b. At low polymer concentration the factor is small, hence making the viscoelastic modes difficult to detect. Experimental results obtained so far have shown that these viscoelastic modes are always well represented in semidilute  $\Theta$  solutions, regardless of polymer and solvent, and they are nearly absent in good and marginal solvents.<sup>31</sup> However the QELS spectra of the present system as well as PS in other good solvents<sup>32</sup> show the ubiquity of the viscoelastic modes. Its presence is not limited to semidilute  $\Theta$  solutions.

Nevertheless, it should be pointed out that the terminal relaxation time of the polymer solution as determined by mechanical measurements is highly molecular weight dependent, but, on the other hand, the QELS spectra of the concentrated polymer solution (or polymer melt) show that the viscoelastic modes are molecular weight independent due mainly to localized segmental dynamics. The study of the molecular weight dependence of the viscoelastic modes for the polymer solution making transition from the semidilute to the concentrated region by QELS will be very fruitful to make the distinction of the two. Work of this nature is presently in progress.

## V. Conclusion

In summary, we have carried out a comprehensive study of the photon correlation function obtained from QELS of PS in DEP as a function of PS concentration and molecular weight. In the semidilute and concentrated concentration regimes, the time correlation function deviates from a single exponential. The deviation is interpreted as arising from two types of modes, one associated with cooperative diffusion whose relaxation rate is proportional to  $q^2$  and the other with a group of relaxation modes associated with the viscoelasticity of the polymer solution. The experimental results are interpreted in terms of a generalized hydrodynamic theory recently developed in this laboratory. With the help of the theory, we have shown how the information regarding the viscoelasticity of the polymer solution can be extracted by the combined use of QELS and static light scattering techniques. We have obtained the osmotic and longitudinal stress moduli, cooperative diffusion coefficient, and friction coefficient as a function of concentration.

**Acknowledgment.** This work is financially supported by the National Science Foundation (Grant DMR 1192993), ONR, and the Center of Material Research and Analysis at the University of Nebraska. Useful technical discussion with Dr. Y. H. Lin and Brillouin scattering measurements by S. Jampani are acknowledged.

## References and Notes

- Wang, C. H.; Fischer, E. W. *J. Chem. Phys.* 1985, 82, 632. Wang, C. H.; Fytas, G.; Fischer, E. W. *Ibid.* 1985, 82, 4332.
- Wang, C. H. *J. Chem. Phys.* 1992, 97, 508.
- Wang, C. H. *J. Chem. Phys.* 1991, 95, 3788.
- Wang, C. H. *Macromolecules* 1992, 25, 1524.
- Berne, B.; Pecora, R. *Dynamic Light Scattering*; Wiley: New York, 1976.
- Munch, J. P.; Candau, S.; Herz, J.; Hild, G. *J. Phys. (Paris)* 1977, 38, 371.
- Geissler, E.; Hecht, A. M. *J. Chem. Phys.* 1976, 65, 103. Geissler, E.; Hecht, A. M. *J. Phys. (Paris)* 1978, 39, 955.
- Nose, T.; Chu, B. *Macromolecules* 1979, 12, 590, 599. Chu, B.; Nose, T. *Macromolecules* 1980, 13, 122.
- Jamieson, A. M.; Reihanian, H.; Southwick, J. G.; Yu, T. L.; Blackwell, J. *Ferroelectrics* 1980, 30, 267.
- Hecht, A. M.; Bohidar, H. B.; Geissler, E. T. *J. Phys. (Paris), Lett.* 1984, 45, L-121.
- Amis, E. J.; Han, C. C.; Matsushita, Y. *Polymer* 1984, 25, 650.
- Takahashi, M.; Nose, T. *Polymer* 1986, 27, 1071.

- (13) (a) Adam, M.; Delsanti, M. *J. Phys. (Paris), Lett.* **1984**, *45*, L-279. (b) Adam, M.; Delsanti, M. *Macromolecules* **1985**, *18*, 1760.
- (14) Brown, W. *Macromolecules* **1986**, *19*, 387, 1083.
- (15) Brown, W.; Johnsen, R. M. *Macromolecules* **1986**, *19*, 2002.
- (16) Nicolai, T.; Brown, W.; Hvidt, S.; Heller, K. *Macromolecules* **1990**, *23*, 5088.
- (17) De Gennes, P.-G. *Macromolecules* **1976**, *9*, 587.
- (18) De Gennes, P.-G. *Scaling Concepts in Polymer Physics*; Cornell University Press: Ithaca, NY, 1979.
- (19) Brochard, F.; de Gennes, P.-G. *Macromolecules* **1977**, *10*, 1157.
- (20) Hwang, D.; Cohen, C. *Macromolecules* **1984**, *17*, 1679, 2890.
- (21) Eisele, M.; Burchard, W. *Macromolecules* **1984**, *17*, 1636.
- (22) Brochard, F. *J. Phys. (Paris)* **1983**, *44*, 39.
- (23) Wang, C. H. In *Dynamic Light Scattering. The Method and Some Applications*; Brown, W., Ed.; Oxford University Press: Oxford, 1992; Chapter 5.
- (24) Equations 23a and 23b of ref 4 should be corrected by multiplying  $M_0$  by  $\beta$  in the denominator. After making the correction, they become equivalent to eqs 15a and 15b of the present paper.
- (25) Provencher, S. W. *Makromol. Chem.* **1979**, *180*, 201.
- (26) Pike, E. R.; Pomeroy, W. R. M.; Vaughan, J. M. *J. Chem. Phys.* **1975**, *62*, 3188.
- (27) Neglecting the  $M_0$  contribution, Vink (*J. Chem. Soc., Faraday Trans. 1* **1985**, *81*, 1725) suggested  $D_c = \phi_1^2(\partial\Pi/\partial\rho_2)/\zeta'$  rather than the traditional expression  $D_c = \phi_1(\partial\Pi/\partial\rho_2)/\zeta$ . The difference between Vink's and the traditional formula lies in the definition of the frictional coefficients  $\zeta$  and  $\zeta'$ . Changing to the definition of  $D_c$  of Vink would result in a change in the definition of the osmotic modulus as  $M_\Pi = \phi_1^2(\partial\Pi/\partial\rho_2)$ , which is not an accepted formula.
- (28) The entries for  $M_\Pi$  and  $M_0$  in Table I at high concentration enclosed in parentheses are extrapolated values due to the difficulty of removing dust in the sample at high concentration.
- (29) Wang, C. H.; Fytas, G.; Zhang, Z. *J. Chem. Phys.* **1985**, *82*, 3405.
- (30) Ferry, J. D. *Viscoelastic Properties of Polymers*, 3rd ed.; Wiley: New York, 1980.
- (31) Brown, W.; Johnson, R. M.; Konak, C.; Dvoranek, L. *J. Chem. Phys.* **1991**, *95*, 8568.
- (32) Zhang, X. Q.; Wang, C. H., unpublished.